Supporting information: Seismic amplitude response to internal heterogeneity of mass-transport deposits

Jonathan Ford[1], Angelo Camerlenghi[1], Francesca Zolezzi[2], and Marilena Calarco[2]

[1]National Institute of Oceanography and Applied Geophysics – OGS, Trieste, Italy
[2]RINA Consulting, Genova, Italy

Correspondence: J. Ford (jford@inogs.it)

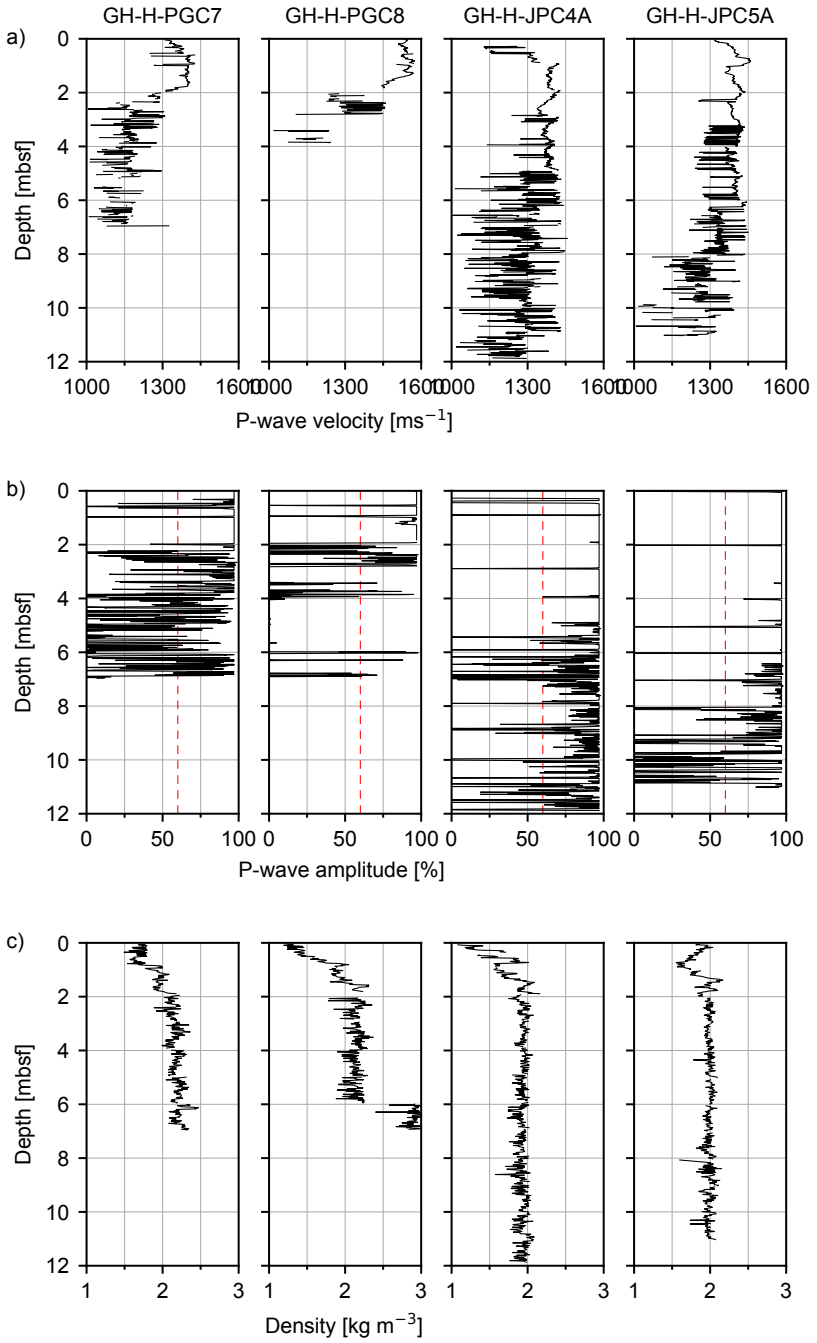

Figure S1. Multi-sensor core logger (MSCL) results from cores GH-H-PGC7, GH-H-PGC8, GH-H-JPC4A and GH-H-JPB5A. a) P-wave velocity, b) P-wave amplitude (60% cutoff marked), c) density, d) cross-plot of P-wave velocity and density logs, for depth intervals where the P-wave amplitude exceeds the 60% cutoff. Parameters for the water layer and the two component sediment lithologies used in the realistic multi-source synthetic experiment (Section 3.2) (cont.)

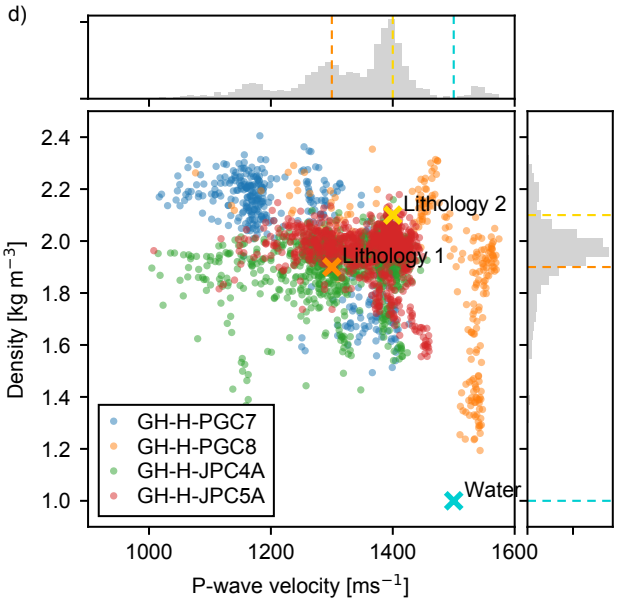
d)
2.4
2.2
2.0
1.8
1.6
1.4
1.2
1.0
Density [kg m^{-3}]
1000
1200
1400
1600
P-wave velocity [ms^{-1}]
Lithology 2
Lithology 1
Water
GH-H-PGC7
GH-H-PGC8
GH-H-JPC4A
GH-H-JPC5A

Figure S1.

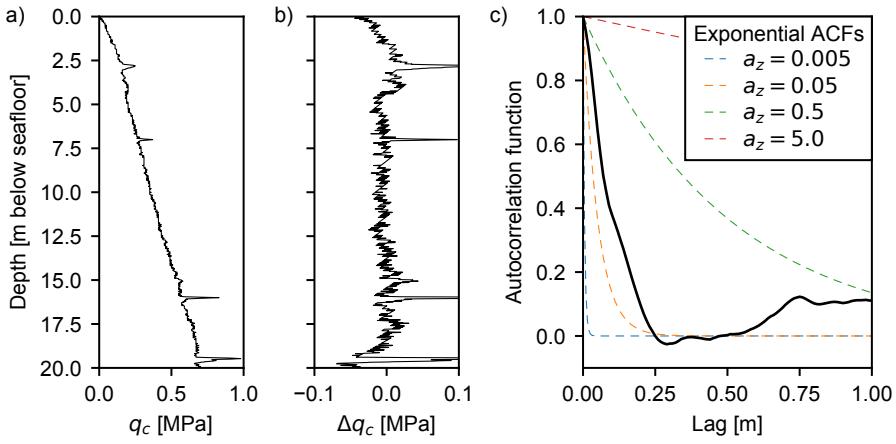

Figure S2. Cone-penetration test (CPT) results for site GH-T-PCPT7. a) Cone-tip resistance (q_c) log, b) De-trended cone-tip resistance log (Δq_c), de-trended with a best fit linear trend, c) Autocorrelation function (ACF) of the cone-tip resistance log.

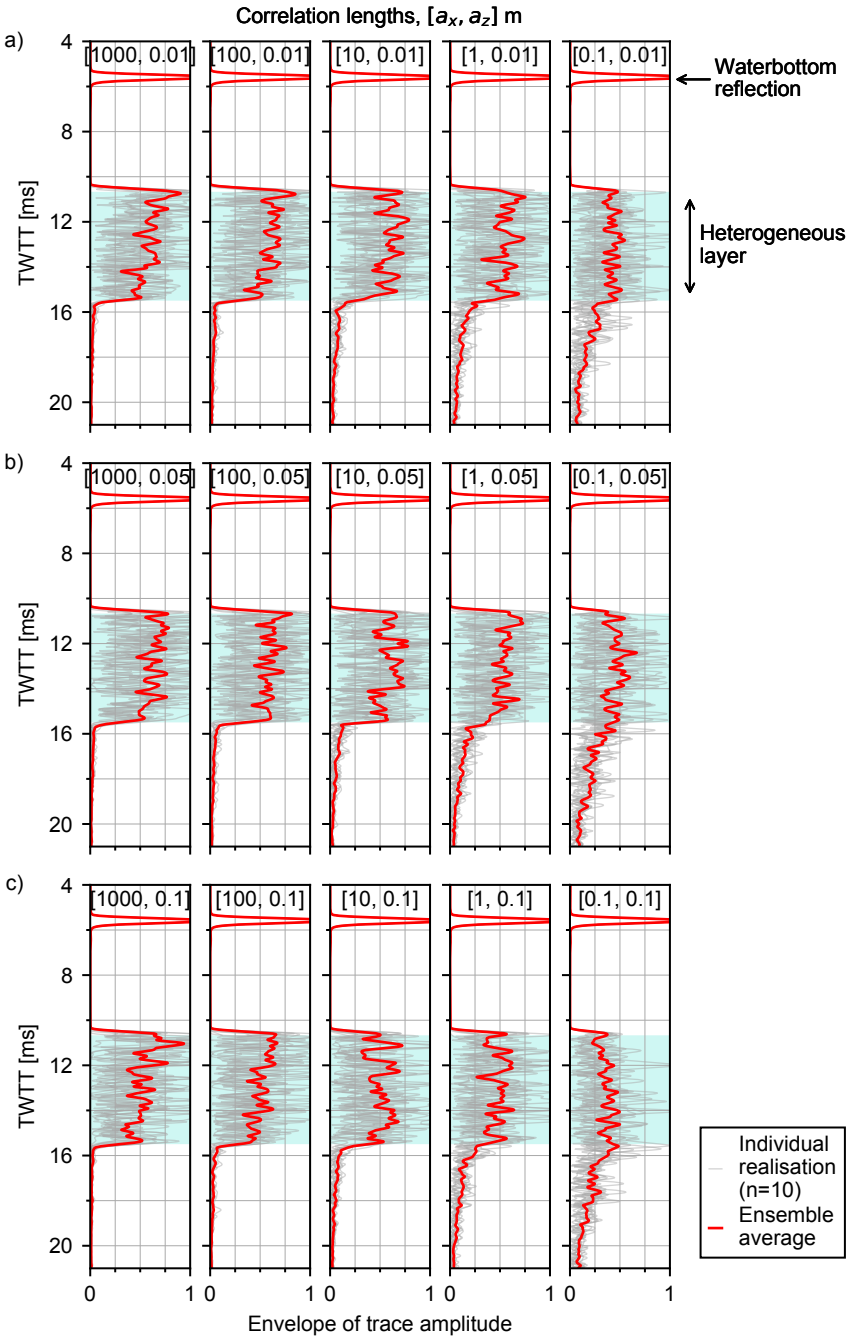

Figure S3. Envelope of trace amplitude for individual realisations (grey) and the RMS envelope of the single-source synthetic experiment for each unique set of correlation lengths (red) for vertical correlation lengths $a_z = \{0.01, 0.05, 0.1, 0.5, 1\}$ m (a-e) and lateral correlation lengths $a_x = \{1000, 100, 10, 1, 0.1\}$ m (left to right). The two-way traveltime (TWTT) extent of the heterogeneous layer is shaded in blue. (cont.)

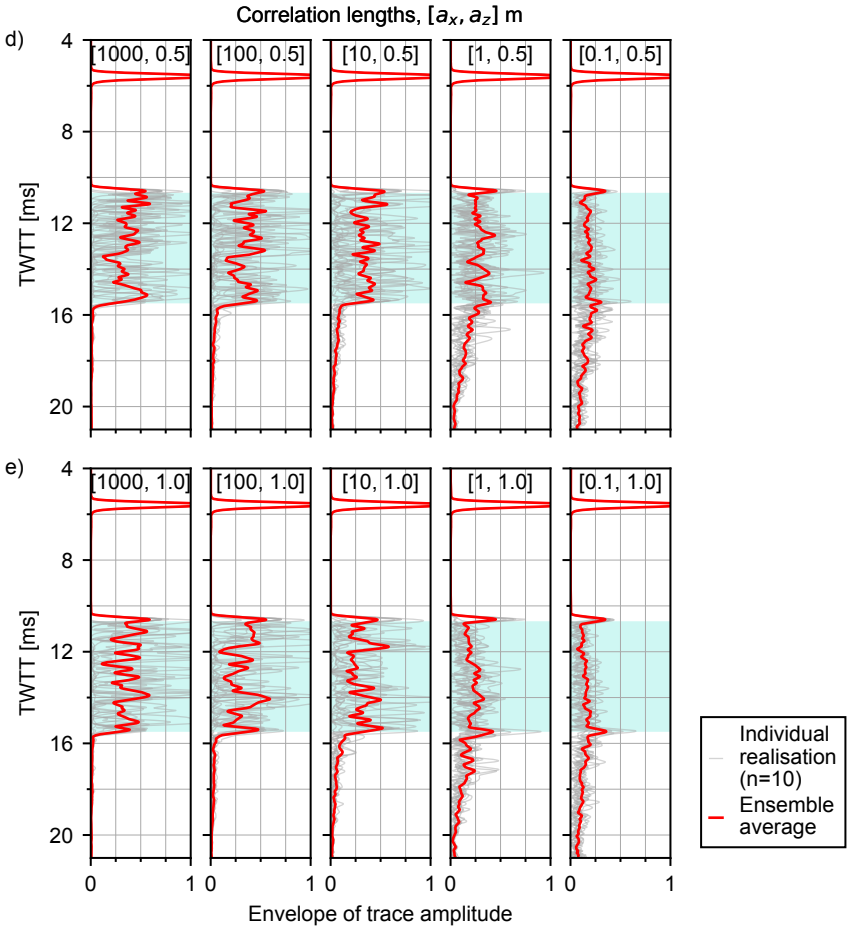
Correlation lengths, [a_x, a_z] m
d)
e)
[1000, 0.5]
[100, 0.5]
[10, 0.5]
[1, 0.5]
[0.1, 0.5]
[1000, 1.0]
[100, 1.0]
[10, 1.0]
[1, 1.0]
[0.1, 1.0]
TWTT [ms]
4
8
12
16
20
0
1
Envelope of trace amplitude
Individual realisation (n=10)
Ensemble average

Figure S3.

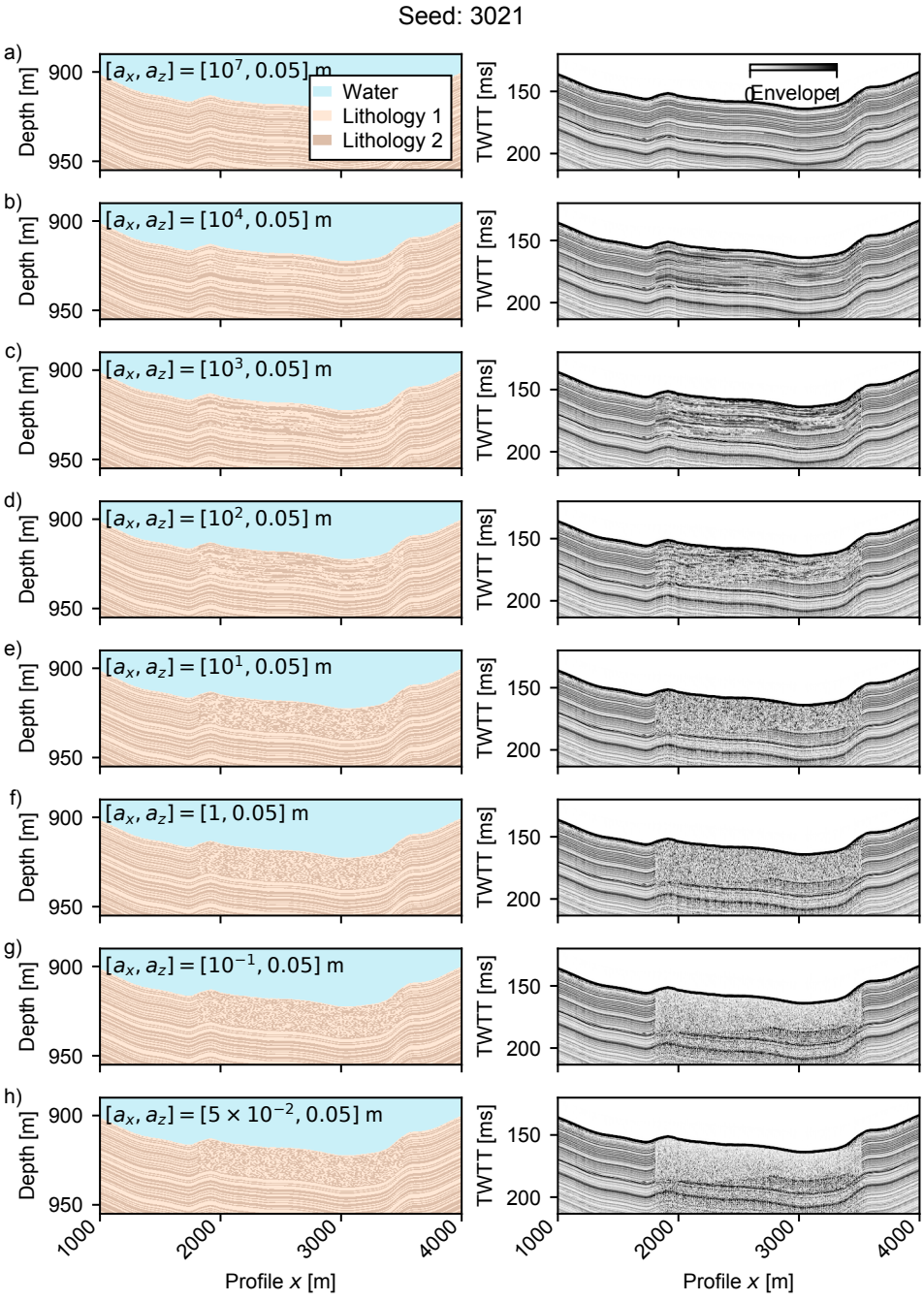

Figure S4. Realisations of the realistic multi-source synthetic experiment models (left) and resulting synthetic sub-bottom profiles (right) for seed 3021, lateral scale lengths $a_x = \{1 \times 10^7, 1 \times 10^4, 1000, 100, 10, 1, 0.1, 0.05\}$ (a-h) and vertical scale length $a_z = 0.05$ m.

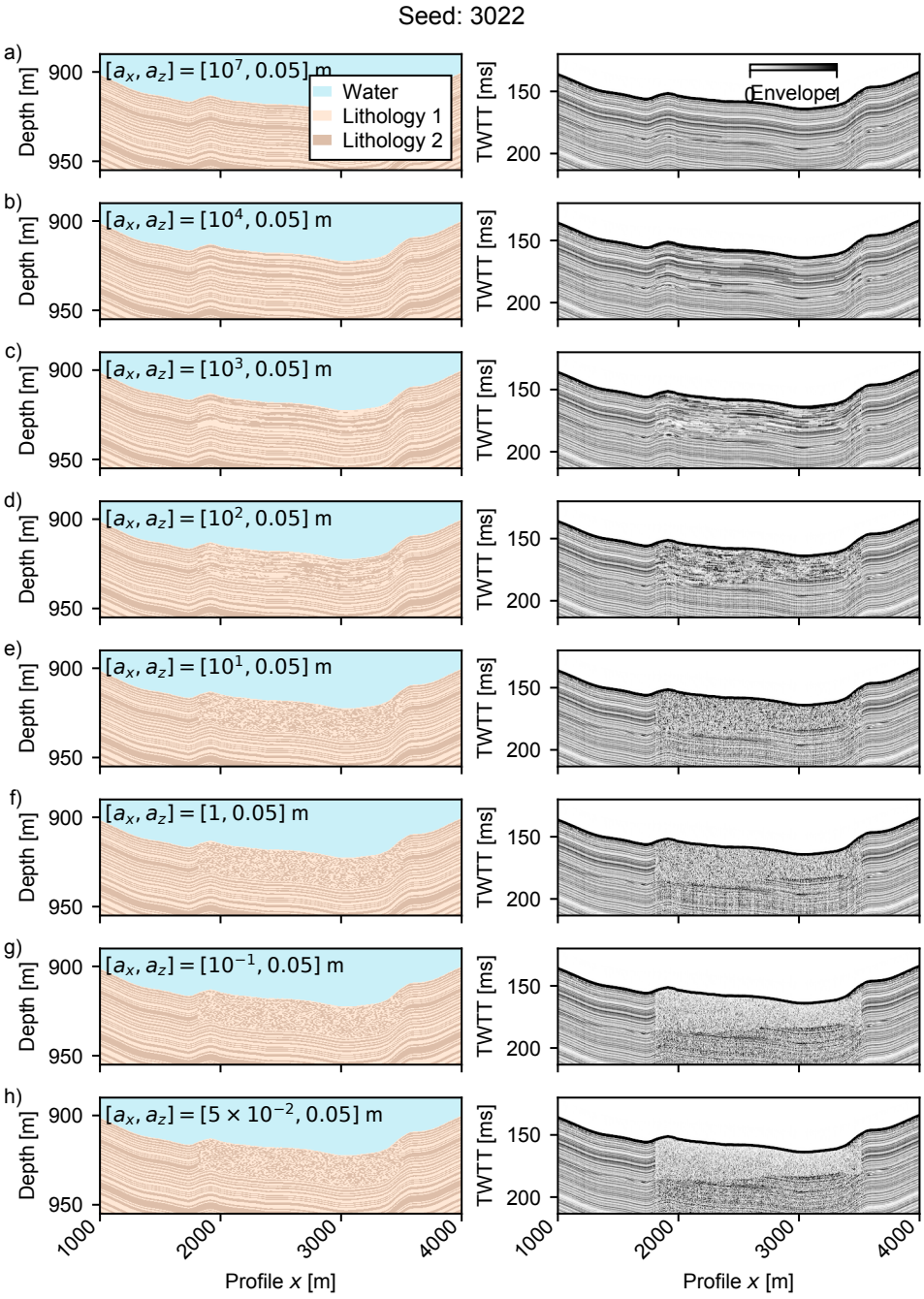

Figure S5. Realisations of the realistic multi-source synthetic experiment models (left) and resulting synthetic sub-bottom profiles (right) for seed 3022, lateral scale lengths $a_x = \{1 \times 10^7, 1 \times 10^4, 1000, 100, 10, 1, 0.1, 0.05\}$ (a-h) and vertical scale length $a_z = 0.05$ m.

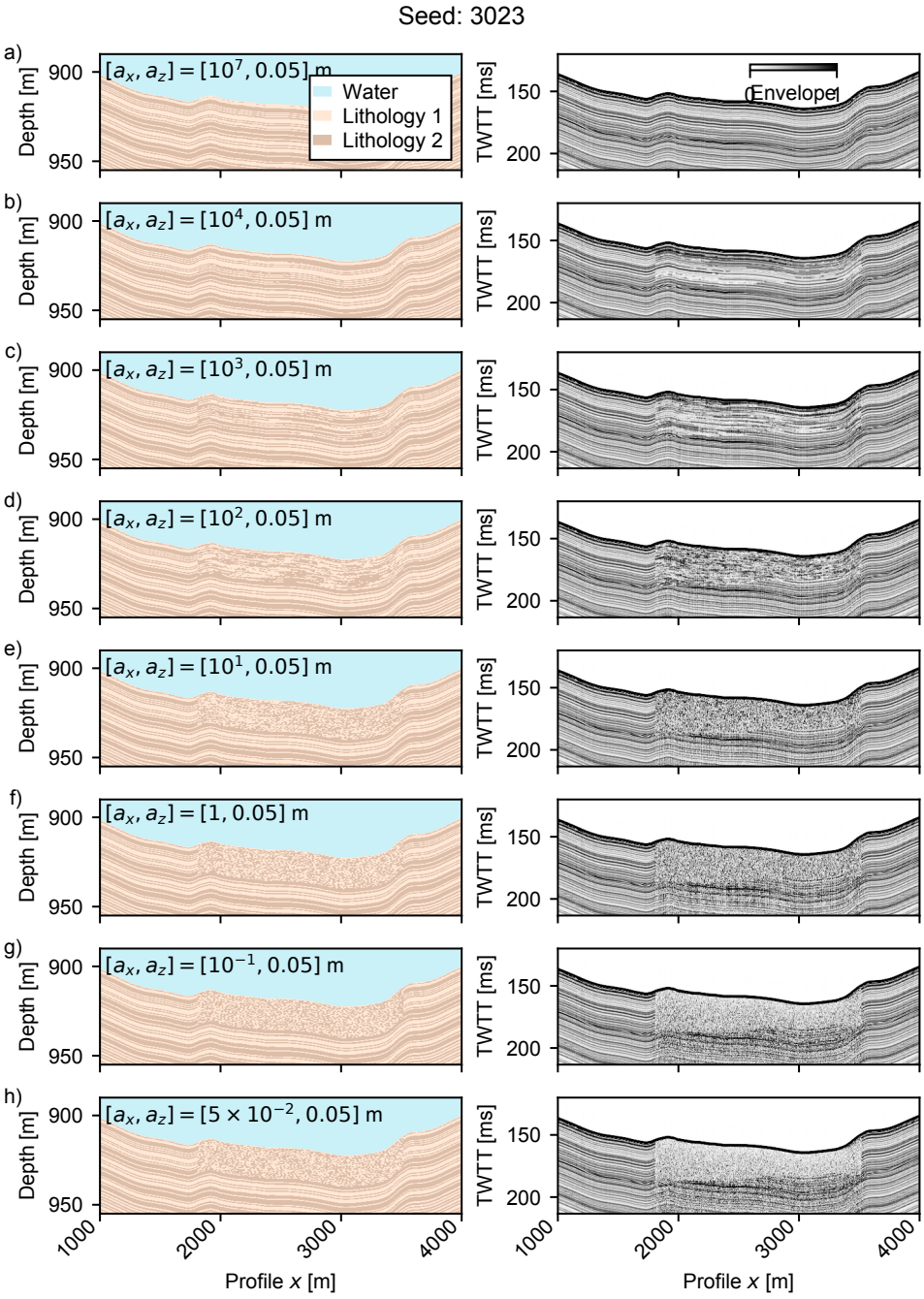

Figure S6. Realisations of the realistic multi-source synthetic experiment models (left) and resulting synthetic sub-bottom profiles (right) for seed 3023, lateral scale lengths $a_x = \{1 \times 10^7, 1 \times 10^4, 1000, 100, 10, 1, 0.1, 0.05\}$ (a-h) and vertical scale length $a_z = 0.05$ m.

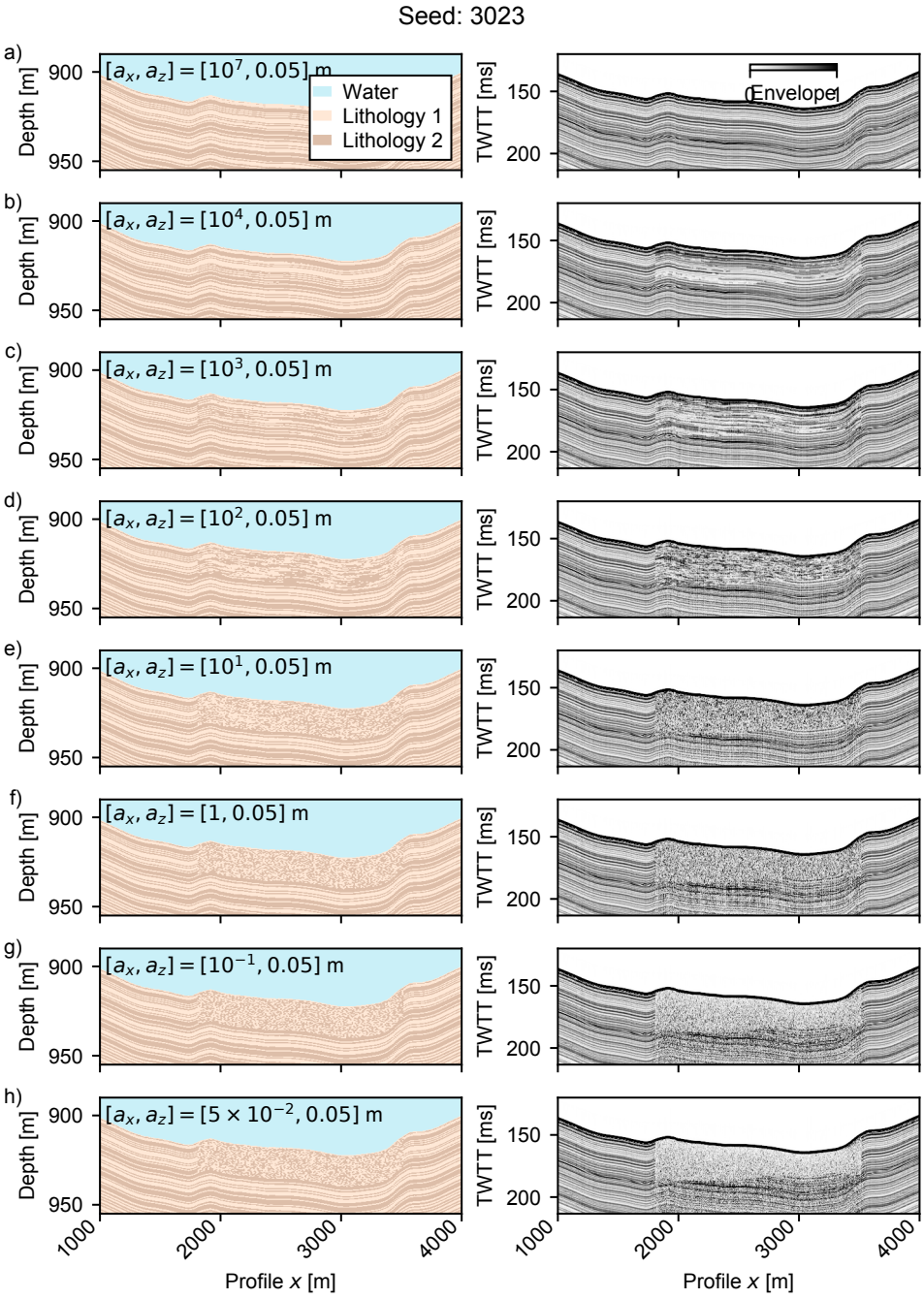

Figure S7. Realisations of the realistic multi-source synthetic experiment models (left) and resulting synthetic sub-bottom profiles (right) for seed 3024, lateral scale lengths $a_x = \{1 \times 10^7, 1 \times 10^4, 1000, 100, 10, 1, 0.1, 0.05\}$ (a-h) and vertical scale length $a_z = 0.05$ m.

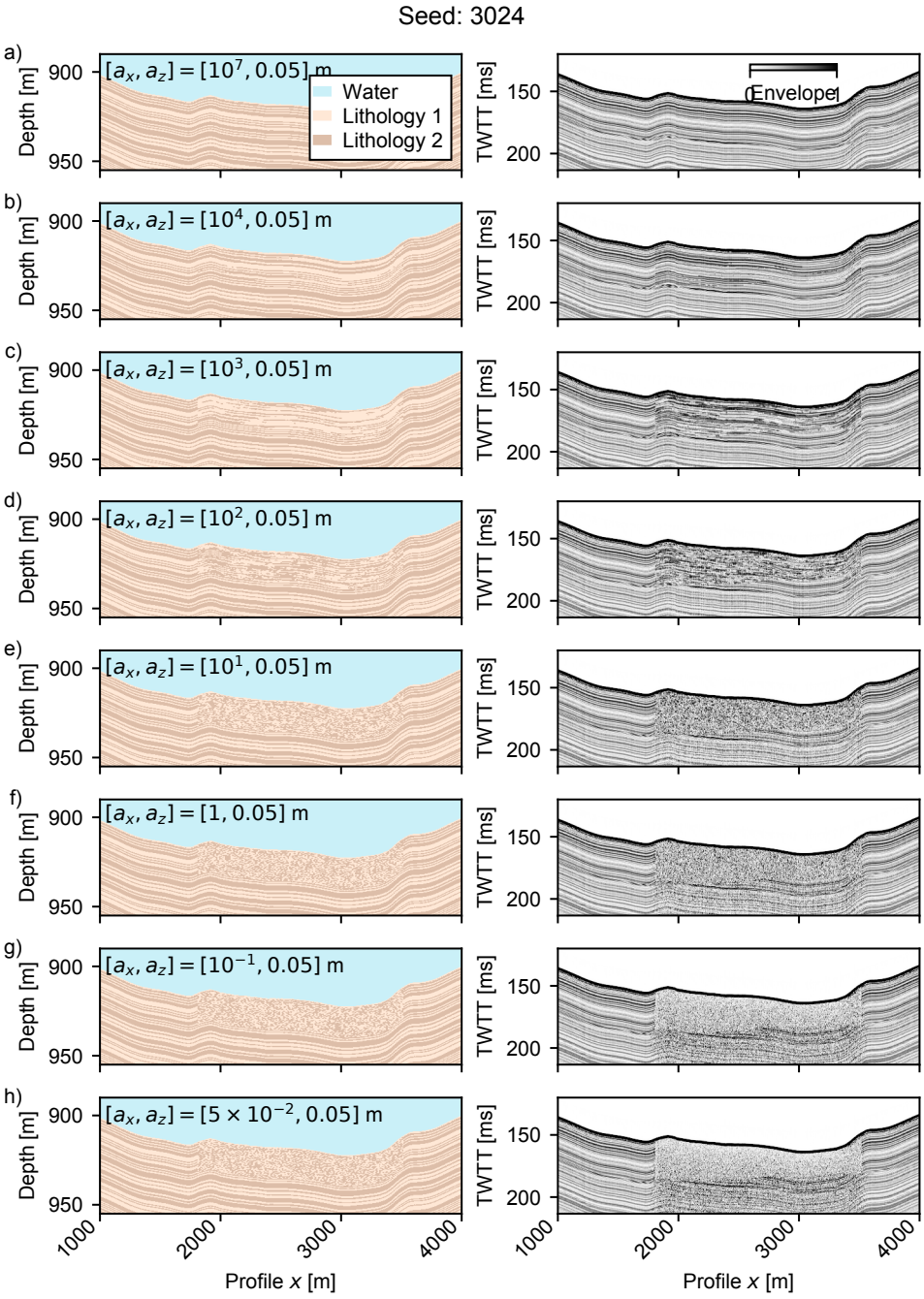

Figure S8. Realisations of the realistic multi-source synthetic experiment models (left) and resulting synthetic sub-bottom profiles (right) for seed 3025, lateral scale lengths $a_x = \{1 \times 10^7, 1 \times 10^4, 1000, 100, 10, 1, 0.1, 0.05\}$ (a-h) and vertical scale length $a_z = 0.05$ m.